One reporter for in-cell activity profiling of majority of protein kinase oncogenes

Iva Gudernova[1], Silvie Foldynova-Trantirkova[2], Barbora El Ghannamova[2], Bohumil Fafilek[1,3], Miroslav Varecha[1,3], Lukas Balek[4], Eva Hruba[1,3], Lucie Jonatova[4], Iva Jelinkova[1,3], Michaela Kunova Bosakova[1], Lukas Trantirek[2], Jiri Mayer[5], Pavel Krejci[1,3]*

[1]Department of Biology, Faculty of Medicine, Masaryk University, Brno, Czech Republic; [2]Central European Institute of Technology, Masaryk University, Brno, Czech Republic; [3]International Clinical Research Center, St. Anne's University Hospital, Brno, Czech Republic; [4]Department of Experimental Biology, Faculty of Sciences, Masaryk University, Brno, Czech Republic; [5]Department of Internal Medicine, Hematology and Oncology, Masaryk University Hospital, Brno, Czech Republic

Abstract In-cell profiling enables the evaluation of receptor tyrosine activity in a complex environment of regulatory networks that affect signal initiation, propagation and feedback. We used FGF-receptor signaling to identify *EGR1* as a locus that strongly responds to the activation of a majority of the recognized protein kinase oncogenes, including 30 receptor tyrosine kinases and 154 of their disease-associated mutants. The *EGR1* promoter was engineered to enhance *trans*-activation capacity and optimized for simple screening assays with luciferase or fluorescent reporters. The efficacy of the developed, fully synthetic reporters was demonstrated by the identification of novel targets for two clinically used tyrosine kinase inhibitors, nilotinib and osimertinib. A universal reporter system for in-cell protein kinase profiling will facilitate repurposing of existing anti-cancer drugs and identification of novel inhibitors in high-throughput screening studies.

DOI: 10.7554/eLife.21536.001

*For correspondence: krejcip@ med.muni.cz

Competing interests: The authors declare that no competing interests exist.

Introduction

Receptor tyrosine kinases (RTKs) form multiprotein complexes at the cell membrane that mediate signal initiation and propagation, as well as feedback control mechanisms (*Lemmon and Schlessinger, 2010*). While cell-free activity profiling may only uncover chemicals that directly target RTK catalytic function, in-cell profiling confers several additional benefits that could improve the drug development process. First, RTKs are targeted in their natural conformation, with post-translational modifications and in the cell metabolic environment. The protein-protein interactions involved in signal transduction through the RTK-associated signaling complexes, downstream elements, or effector pathways may also be targeted, increasing the chance of success. In-cell profiling may identify biological pathways that naturally oppose the signaling of a certain RTK, and can then be therapeutically exploited (*Wendt et al., 2015*). Furthermore, this approach may also enable the targeting of RTKs in non-signaling states, via interference either with their expression, maturation and transport to the cell membrane or their internalization and degradation. Finally, in-cell activity profiling is applicable to disease-specific in vitro and in vivo models. This is important in the development of therapeutics for chronic diseases caused by pathological RTK signaling, such as diabetes, pulmonary hypertension, chronic kidney disease, or developmental disorders (*Fountas et al., 2015*; *ten Freyhaus et al., 2012*; *Harskamp et al., 2016*; *Laederich and Horton, 2012*), all of which are

poorly represented in current clinic (*Bamborough, 2012*). Lastly, several important oncogenes and downstream targets of RTK signaling, such as RAS, appear not druggable directly (*Cox et al., 2014*) and thus the inhibitors of their signaling may only be discovered via in-cell activity profiling. However, the existing toolkits for in-cell RTK activity profiling provide only partial solutions for the development of RTK inhibitors, as they only focus on a few RTKs or their disease-associated mutants (*Supplementary file 1A*), are technically or instrumentally challenging, or require the development of RTK-specific tools (*Ni et al., 2006*; *Inglés-Prieto et al., 2015*; *Regot et al., 2014*).

A majority of known RTKs activate the RAS/RAF/MEK/ERK MAP kinase signaling module, a pathway that links extracellular mitogenic signals to gene transcription (*Vogelstein et al., 2013*; *Meloche and Pouysségur, 2007*). Hence, the strong effect of ERK on gene transcription could be exploited in the development of reporters that are applicable to the activity profiling of many different RTKs (*Yang et al., 2003*). Here, we report the engineering of one such system, which is based on the promoter sequences of the ERK target gene *EGR1* (*Early growth response 1*). We demonstrate that the *EGR1*-based reporter system is applicable to simple in-cell activity profiling of most protein kinase oncogenes. Additionally, we generate proof-of-concept examples for the use of this system in the identification of novel targets for clinically used protein kinase inhibitors.

Results and discussion

Exploitation of the *EGR1* for the activity profiling of fibroblast growth factor receptor (FGFR)

We focused on the particularly strong ERK activation triggered by FGFR signaling in multiple myeloma and rat chondrosarcoma (RCS) cells to identify genes which are upregulated upon ERK activation. The expression profiling of cells treated with FGFR ligand FGF2 identified *Egr1*, *Egr2*, *Nr4A2*, *Dusp6* and *Rgs1* among the most strongly induced genes (*Krejci et al., 2010*; *Buchtova et al., 2015*). The putative promoter sequences of human *EGR1*, *EGR2*, *NR4A2*, *DUSP6* and *RGS1*, located directly upstream of the transcription start sites (*Supplementary file 1B*), were cloned into the promoterless pGL4.17 vector carrying firefly luciferase. In dual-luciferase activity assays performed in RCS cells, *EGR1* promoter showed the strongest response, as it was *trans*-activated approximately 12-fold following FGF2 treatment (*Figure 1A*), and was therefore chosen for subsequent studies. FGF2 induced endogenous EGR1 protein expression in seven different cell types tested, and this phenotype was dependent on ERK activation (*Figure 1A*; *Figure 1—figure supplement 1*).

To identify FGF2-responsive elements, we generated 13 truncated variants of the 2112nt-long human *EGR1* promoter that had originally been cloned into the pGL4.17 vector (−1951/+161 relative to the transcription start site; TSS) (*Figure 1—figure supplement 2*), and subjected these variants to FGF2-mediated *trans*-activation in a dual-luciferase assay (*Figure 1—figure supplement 3*). Four successive rounds of 3- and/or 5-prime sequence shortening and optimization identified a 402nt-long region (−799/–397 relative to TSS) that is critical for FGF2-mediated *trans*-activation (called D-E element) of the *EGR1* promoter (*Figure 1B–D*; *Figure 1—figure supplement 2*). The addition of two extra copies of the D-E element into the *EGR1* promoter (hEGR1-D) enhanced its response to FGF2 by approximately 50% (*Figure 1E*). We named this construct pKrox24(2xD-E_inD)^{Luc} after KROX24, one of the alternative names of EGR1 (*Supplementary file 1C*). The level of pKrox24(2xD-E_inD)^{Luc} FGF2-mediated *trans*-activation in RCS cells peaked at approximately 40 ng/ml FGF2. Treatment of RCS cells with higher doses of FGF2 further elevated ERK activation (*Krejci et al., 2007*), but had a negligible effect on pKrox24(2xD-E_inD)^{Luc} activity (*Figure 1—figure supplement 4*), implying that it is unlikely that further development of the pKrox24(2xD-E_inD)^{Luc} promoter sequence would yield a significant increase in trans-activation capacity. In the five different cell types tested, pKrox24(2xD-E_inD)^{Luc} responded to the activation of FGFR signaling following FGF2 addition, as well as to the chemical inhibition of endogenous FGFR signaling (*Figure 1—figure supplement 5*).

To eliminate inhibitory elements possibly existing within the pKrox24(2xD-E_inD)^{Luc} promoter, a fully synthetic construct was developed, based on *EGR1* promoter and information gained during the pKrox24 development. A human *EGR1* promoter sequence (−1500/+100 bp relative to TSS) was aligned with the corresponding sequences of pig, cow, rat, mouse and chicken *Egr1*, and analyzed by T-Coffee (*Notredame et al., 2000*) to find conserved elements, and by rVista (*Loots and*
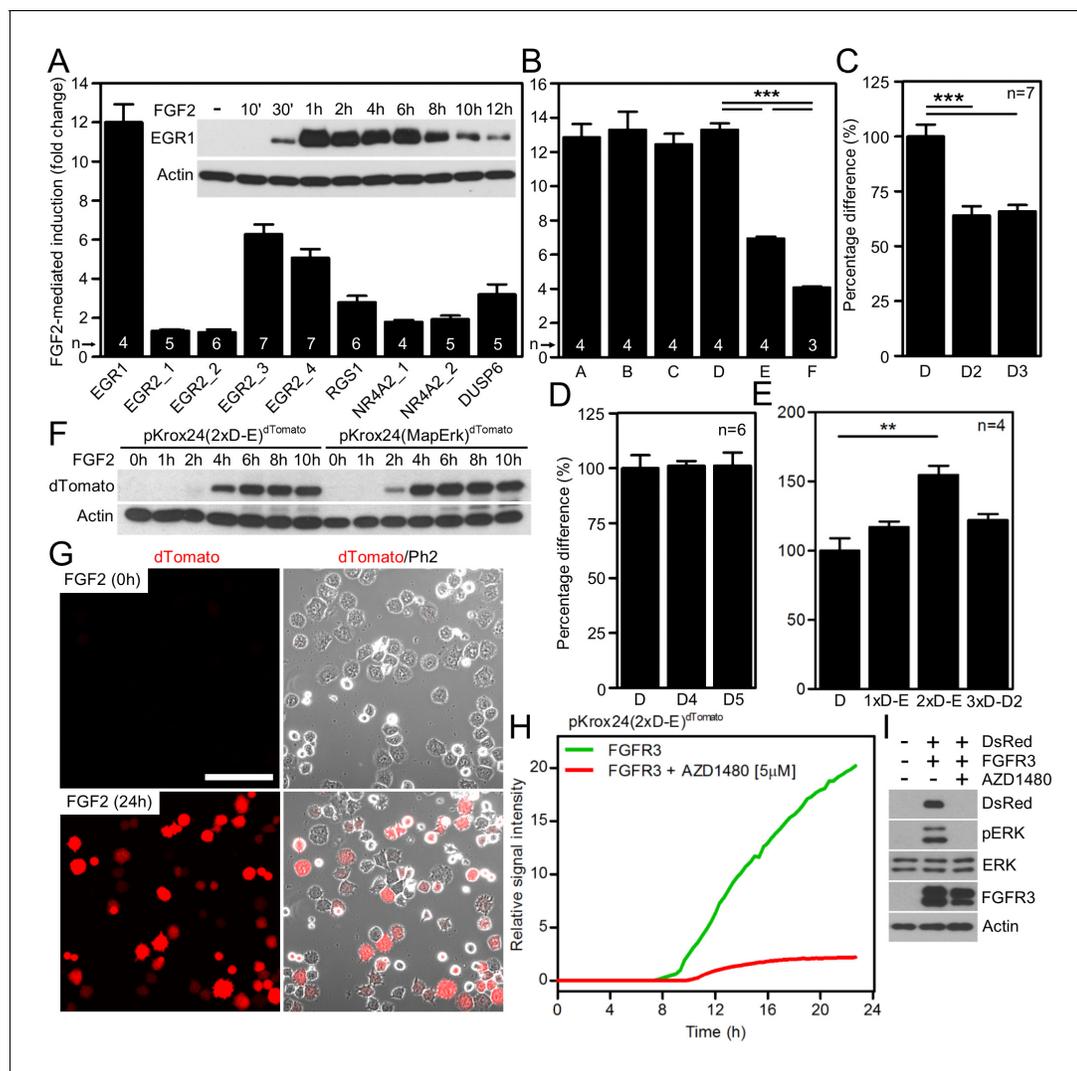
Figure 1. Development of luciferase and fluorescent reporters based on a human *EGR1* promoter. (**A**) The activity of various reporters, based on promoters of FGF2-responsive genes, cloned into a pGL4.17 vector expressing firefly luciferase. The FGF2-mediated *trans*-activation (fold-change compared to unstimulated cells) of these reporters in RCS cells was determined by the dual-luciferase assay. Insert, induction of EGR1 protein expression in RCS cells treated with FGF2. (**B–E**) Four consecutive rounds of *EGR1* promoter sequence optimization leading to the pKrox24(2xD-E_inD)^{Luc} reporter, including 5'-prime shortening (**B,C**), 3'-prime shortening (**D**), and addition of repetitive D-elements (**E**) to the originally cloned *EGR1* promoter (vectors outlined in *Figure 1—figure supplement 2*). The presented data were generated through dual-luciferase assays in RCS cells, with 'n' describing the number of independent experiments. Statistically significant differences are highlighted (Student's t-test; **p<0.01, ***p<0.001). (**F, G**) FGF2-mediated induction of dTomato protein expression (**F**) and fluorescence (**G**) in RCS cells transiently transfected with pKrox24(2xD-E)^{dTomato} or pKrox24(MapErk)^{dTomato} reporters. Bar, 150 µm. (**H**) Transactivation of pKrox24(2xD-E)^{dTomato} in RCS cells induced by forced expression of the constitutively active FGFR3 K650M mutant, determined by live cell imaging of dTomato fluorescence over 24 hr. The dTomato induction was suppressed by the FGFR inhibitor AZD1480. (**I**) Immunoblot validation of DsRed induction and ERK phosphorylation (p) in RCS cells transfected with FGFR3 K650M mutant together with pKrox24(2xD-E)^{DsRed} for 16 hr. Actin and total ERK levels served as loading controls.

DOI: 10.7554/eLife.21536.002

The following figure supplements are available for figure 1:

Figure supplement 1. FGF2 induces EGR1 expression dependent on ERK MAP kinase.
DOI: 10.7554/eLife.21536.003

Figure supplement 2. Schematic outline of human *EGR1* promoter sequences cloned into the promoterless pGL4.17 vector carrying firefly luciferase, and analyzed for FGF2-mediated *trans*-activation as shown by *Figure 1A–E*.
DOI: 10.7554/eLife.21536.004

Figure supplement 3. Analysis workflow of the dual-luciferase assay.
DOI: 10.7554/eLife.21536.005

Figure 1 continued on next page

Figure 1 continued

Figure supplement 4. The extent of pKrox24(2xD-E_inD)^Luc reporter *trans*-activation with increasing FGF2 concentrations in RCS cells.
DOI: 10.7554/eLife.21536.006

Figure supplement 5. Validation of pKrox24(2xD-E_inD)^Luc reporter in cellular models to FGFR signaling.
DOI: 10.7554/eLife.21536.007

Figure supplement 6. Generation of pKrox24(MapErk) reporters.
DOI: 10.7554/eLife.21536.008

Figure supplement 7. Comparison of transactivation capacity and basal activity of pKrox24(MapErk)and pKrox24(2xD-E_inD) reporters.
DOI: 10.7554/eLife.21536.009

Figure supplement 8. FGF-mediated transactivation of constructs containing D-E or MapErk promoter elements combined with dTomato or DsRed reporters.
DOI: 10.7554/eLife.21536.010

Ovcharenko, 2004) to identify transcription factor binding sites. The identified elements, together with previously discovered sequences (*Wang et al., 2010*), were mapped onto the *EGR1* promoter and cloned into a pGL4.26 vector containing a minimal promoter and firefly luciferase. The resulting reporter was named pKrox24(MapErk)^Luc (*Figure 1—figure supplement 6*). When compared to pKrox24(2xD-E_inD)^Luc, pKrox24(MapErk)^Luc showed no additional increase in FGF2-mediated *trans*-activation, but possessed a significantly lower basal activity in RCS and 293T cells (*Figure 1—figure supplement 7*).

Additionally, constructs containing five copies of MapErk or two copies of D-E elements, serving as minimal promoters, were generated with either dTomato or DsRed reporter (*Supplementary file 1C*). These reporters responded well to FGF2-mediated *trans*-activation following transfection into RCS cells, shown by immunoblot analyses of dTomato and DsRed expression, and live cell imaging (*Figure 1F,G*; *Figure 1—figure supplement 8*). Expression of the constitutively active FGFR3 mutant K650M (*Naski et al., 1996*) in RCS cells induced dTomato or DsRed expression, and this expression was reversed by treatment with AZD1480, a chemical inhibitor of FGFR3 (*Scuto et al., 2011*) (*Figure 1H,I*; *Figure 1—figure supplement 8C*).

Protein kinases induce EGR1 protein expression in cells

Next, we investigated whether RTKs other than FGFRs induce EGR1 expression in cells. A total of 37 full-length human wild-type (wt) RTKs were cloned into the pcDNA3.1 vector in frame with a C-terminal V5/6xHis epitope, expressed in 293T cells, and verified by immunoblot (*Figures 2* and *3*). Site-directed mutagenesis was used to generate the major mutants of each RTK associated with human disease, obtained via surveys of published literature, or selected from the catalogue of mutations associated with human cancers or inherited conditions available from the Sanger Cosmic (*Forbes et al., 2015*) and OMIM databases. As RTKs auto-phosphorylate upon activation (*Bae and Schlessinger, 2010*), a phosphorylation-specific RTK antibodies were used to estimate the spontaneous or ligand-induced activation of expressed RTKs (*Figures 2* and *3*; *Supplementary file 1D*). A total of 254 wt and mutant RTK variants were prepared this way, expressed in 293T cells, and analyzed for EGR1 induction. The results showed that 30 wt RTKs (81%) and 154 (71%) of their mutants induced EGR1 when expressed in 293T cells (*Figure 4*).

Three wt RTKs (FGFR3, TIE, VEGFR1) and 27 mutants induced EGR1 expression but were not found to be phosphorylated (*Figures 2–4*). This is likely due to the fact that in active RTKs some phosphotyrosines are differentially phosphorylated and thus may not be identified by antibodies designed for specific motifs. The most notable example is FGFR3, as all five active mutants associated with skeletal dysplasia and cancer (*Kant et al., 2015*; *Passos-Bueno et al., 1999*; *Carter et al., 2015*) induced EGR1, but only K650M FGFR3 was found to be phosphorylated by an antibody recognizing FGFR phosphorylation at Y653/Y654. The pseudokinases lacking catalytic activity (ROR1, ROR2, RYK, ERBB3) were among the RTKs that did not induce EGR1, along with RTKs that did not autophosphorylate after expression in 293T cells (TYRO3, INSRR, ROS1) (*Figures 2* and *3*). Furthermore, 36 mutants failed to induce EGR1 despite being derived from RTKs that induce EGR1 expression. The majority of these mutants (83%) were kinase-inactive mutants (*Figures 2–4*). The remaining six mutants did not induce EGR1 because of weak activation (DDR1^R896Q, ERBB4^E836K, RET^E768N) or due to an unknown reason (RON^R470C, RON^R1231C, PDGFRB^D850N). Overall, the RTK activation
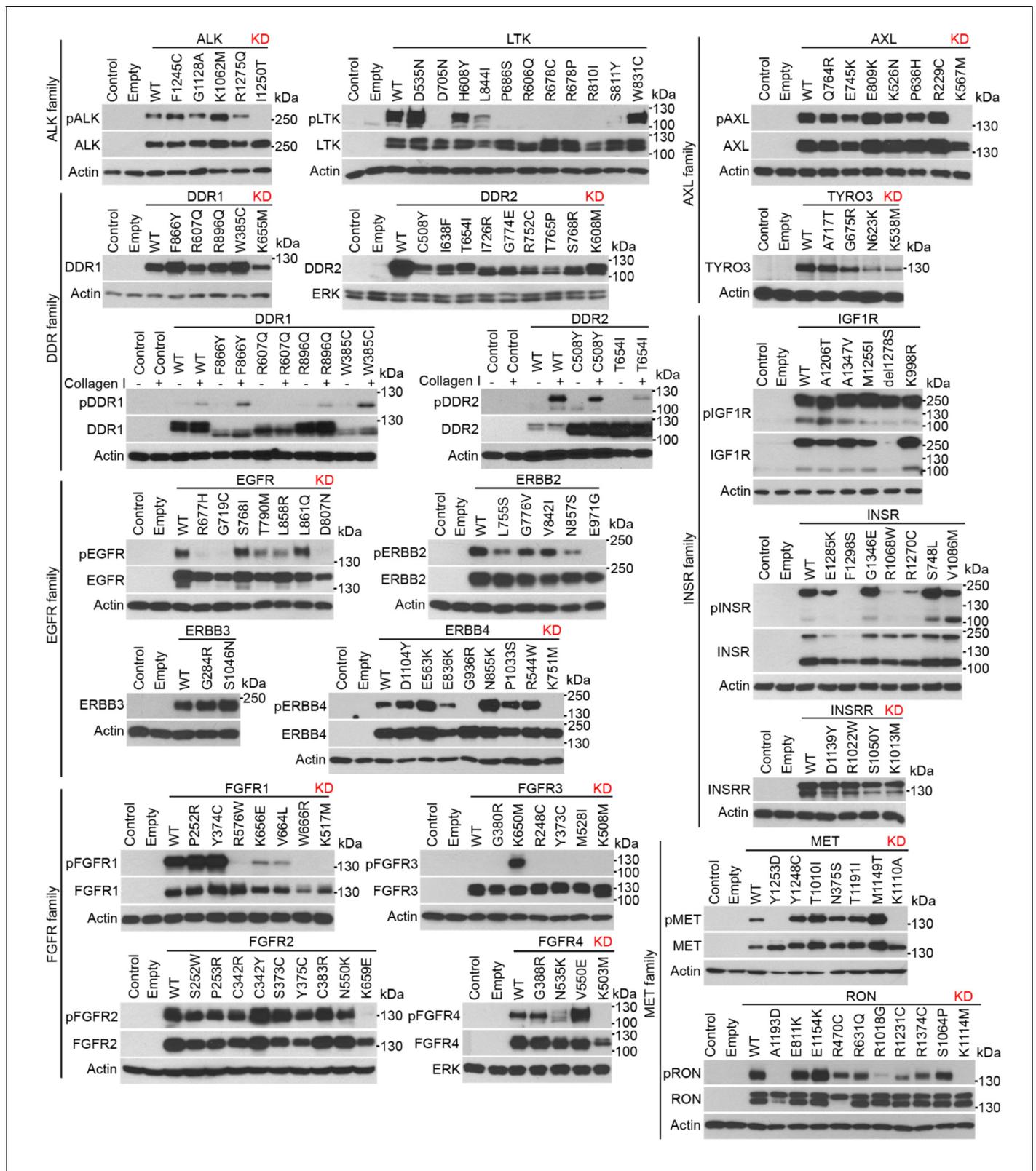
Figure 2. RTK cloning and validation (part 1). Full-length human RTK cDNA was cloned into pcDNA3.1 vectors and equipped with a C-terminal V5/His epitope. Mutants were created by site-directed mutagenesis. The RTKs were expressed in 293T cells, and their activation was probed by immunoblot with antibodies that recognize the given RTK only when it is phosphorylated (p) at a specific motif, with exception of phosphorylated DDR1 and DDR2 which were detected with pan-pY antibody. A total of 37 wild-type (WT) RTKs and 241 of their mutants were obtained, including disease-associated

Figure 2 continued on next page

correlated with EGR1 induction in 96% (154 out of 160) of the tested wt and mutant RTKs. Thirteen additional non-receptor tyrosine kinases, serine/threonine kinases C-RAF and B-RAF as well as RAS small GTPase, were subjected to the same analyses (*Figure 4—figure supplement 1*). Taken together, we have demonstrated that, apart from the JAK and MAPKK kinases not evaluated in this study, all of the protein kinase oncogenes recognized to date (*Vogelstein et al., 2013*) are capable of inducing EGR1 expression in 293T cells.

pKrox24 reporters can be used to identify novel targets for clinically used kinase inhibitors

One application of pKrox24 reporters is the identification of novel targets for clinically used kinase inhibitors, which could help repurpose existing anti-cancer drugs or uncover the molecular mechanisms underlying the side-effects they cause in patients. Chronic myeloid leukemia (CML) is a clonal myeloproliferative disorder characterized by a t(9;22)(q34;q11) translocation that produces a cytoplasmic BCR-ABL fusion protein with constitutive tyrosine kinase activity (*Zhao et al., 2002*). The suppression of BCR-ABL catalytic activity with tyrosine kinase inhibitors (TKI) has greatly improved CML prognosis, effectively turning a once fatal cancer into a manageable chronic disease. Several generations of BCR-ABL TKIs have been developed to improve efficacy and overcome the BCR-ABL resistance to first generation TKIs caused by mutations and gene amplifications (*Hochhaus et al., 2008*; *Cortes et al., 2013*). However, some TKIs, such as ponatinib, can cause severe toxicity in CML patients and even lead to discontinuation of the therapy (*Modugno, 2014*). The reasons why these BCR-ABL TKI side-effects occur are not clear, and in this way, the elucidation of how TKIs affect physiological tyrosine kinase signaling is of major interest to CML research. To identify novel targets, we evaluated the activity of five clinically used BCR-ABL TKIs, that is ponatinib, imatinib, dasatinib, bosutinib and nilotinib, against a panel of 28 wt RTKs. Different TKI concentrations were used to assess the inhibition of BCR-ABL activity as well as cell toxicity (*Figure 5—figure supplement 1A*). *Figure 5A* shows that all tested TKIs inhibited RTKs that had already been reported as targets in literature (*Supplementary file 1E*), with exception of LTK and INSR, which were identified as two novel targets for nilotinib (*Figure 5A*; *Figure 5—figure supplement 1E*).

Osimertinib (AZD9291) is recently described inhibitor of EGFR catalytic activity, and was approved for clinical use in lung carcinoma in 2015 (*Cross et al., 2014*; *Greig and Approval, 2016*). Osimertinib is a mutant-selective EGFR inhibitor, with 200-fold selectivity for EGFR mutants T790M and L858R over the wt EGFR (*Cross et al., 2014*; *Finlay et al., 2014*; *Jiang and Zhou, 2014*). Crystallographic studies indicate that osimertinib binds to the outer edge of the EGFR ATP binding pocket through a covalent bond with Cys797 (*Yosaatmadja et al., 2015*). Although these data provide no clear explanation for EGFR mutant versus the wt selectivity (*Cross et al., 2014*; *Finlay et al., 2014*; *Jiang and Zhou, 2014*; *Yosaatmadja et al., 2015*), osimertinib is expected to possess a very narrow spectrum of RTK specificity, limited to EGFR and the closely related ERBB2 and ERBB4. We tested this prediction by evaluating osimertinib activity against 30 wt RTKs and 116 of their active mutants with a pKrox24(2xD-E_inD)^{Luc} luciferase assay in 293T cells. We observed inhibitory activity for osimertinib against EGFR, ERBB2 and ERBB4, but not for the other 26 RTKs and 99 mutants (*Figure 5B*). However, LTK was an exception, as it appeared to be inhibited by osimertinib in both wt and mutant forms. These included the D535N and L844I mutants, which associate with multiple myeloma and stomach carcinoma (*Hucthagowder et al., 2012*; *Kubo et al., 2009*), respectively, and the W831C and H608Y substitutions found in the Cosmic and VarSome databases. The osimertinib activity was confirmed by suppression of the autophosphorylation of LTK expressed in 293T cells, and by inhibition of LTK-mediated phosphorylation of recombinant STAT1 substrate in cell-free kinase assays (*Figure 5C*).

The presented pKrox24 technology enables rapid in-cell profiling of a majority of the known protein kinase oncogenes via simple and versatile reporters based on the activity of a downstream protein kinase signaling target. While the luciferase reporters may be applied to tractable cell models
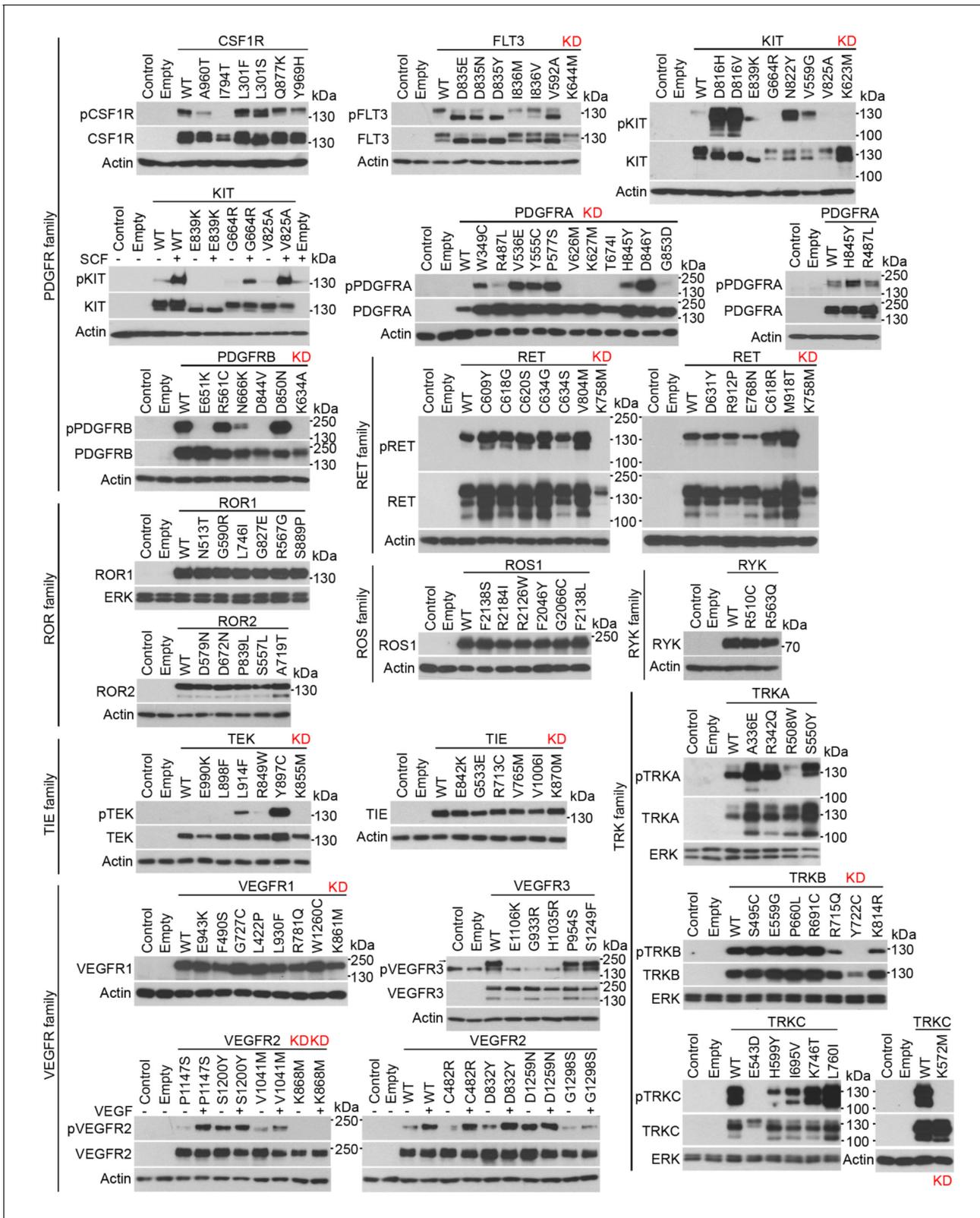
Figure 3. RTK cloning and validation (part 2).
DOI: 10.7554/eLife.21536.012

A

RTK	WT	Mutants
ALK	+	K1062M G1128A F1245C R1275Q
LTK	+	D535N R606Q H608Y R678C* R678P P686S D705N R810I S811Y W831C L844I
AXL	+	R229C K526N P636H E745K Q764R E809K
TYRO3	+	N623K G675R A717T
DDR1	+L	W385CL R607QL F866YL R896QL¶
DDR2	+L	C580YL I638FL T654IL I726RL G774EL R752CL T765PL S768RL
EGFR	+	R677H* G719C S768I T790M L858R L861Q
ERBB2	+	L755S G776V V842I N857S E971G
ERBB3	+	G284R S1046N
ERBB4	+	R544W E563K E836K¶ N855K G936R P1033S D1104Y
FGFR1	+	P252R Y374C R576W* K656E V664L W666R
FGFR2	+	S252W P253R C342R C342Y S373C Y375C C383R N550K K659E*
FGFR3	+*	R248C* Y373C* G380R* M528I* K650M
FGFR4	+	G388R N535K V550E
IGF1R	+	K998R A1206T M1255I d1278S A1347V
INSR	+	S748L R1068W* V1086M R1270C E1285K F1298S* G1346E
INSRR	+	R1022W S1050Y D1139Y
MET	+	N375S T1010I M1149T T1191I Y1248C* Y1253D
RON	+	R470C¶ R631Q E811K R1018G S1064P E1154K A1193D R1231C¶ R1374C
CSF1R	+	L301F L301S I794T* Q877K A960T Y969H
FLT3	+L	V592A D835E D835N D835Y I836ML I836VL
KIT	+L	V559G G664RL D816H D816V N822Y V825AL E839KL
PDGFRA	+	W349C R487L V536E Y555C P577S V626M* T674I H845Y D846Y G853D
PDGFRB	+	E651K R561C N666K D844V D850N¶
RET	+	C609Y C618G C618R C620S D631Y C634G C634S E768N¶ V804M R912P M918T
ROR2	+	S557L D579N D672N A719T P839L
ROS1	+	F2046Y G2066C R2126W F2138L F2138S R2184I
RYK	+	R510C R563Q
TEK	+	R849W* Y897C L898F* L914F E990K*
TIE	+*	G533E* R713C* V765M* E842K* V1006I*
TRKA	+	A336E R342Q R508W S550Y
TRKB	+	S495C E559G P660L R691C R715Q K814R
TRKC	+	E543D H599Y I695V K746T L760I
VEGFR1	+*	L422P* F490S* G727C* R781Q* L930F* E943K* W1260C
VEGFR2	+L	C482RL D832YL V1041ML P1147SL S1200YL D1259NL G1298SL
VEGFR3	+	G933R P954S H1035R E1106K S1249F

Figure 4. RTKs induce EGR1 protein expression. (A, B) Immunoblot analyses of EGR1 induction in 293T cells transfected with wild-type (WT) or mutated RTKs for 24 hr. Cells transfected with empty plasmids serve as the transfection control, and actin serves as the loading control. (A) Green, RTK induces EGR1; red, no EGR1 induction by the RTK; * RTKs that induced EGR1 but were not autophosphorylated (*Figures 2* and *3*); ¶ RTKs that were autophosphorylated but did not induce EGR1; L RTKs activated by the addition of their cognate ligands.

DOI: 10.7554/eLife.21536.013

The following figure supplement is available for figure 4:

Figure supplement 1. EGR1 expression induced by non-receptor tyrosine kinases, serine/threonine kinases C-RAF and B-RAF, and RAS small GTPase.
DOI: 10.7554/eLife.21536.014

to repurpose existing protein kinase inhibitors, the application of fluorescent pKrox24 reporters to high-throughput screening (HTS) of compound libraries offers a major advantage. Cells can be viewed any time during the screening, and this characteristic of HTS would enable researchers to detect false-positive hits based on the inhibition of dTomato and DsRed expression by cell-toxic compounds through mechanisms unrelated to the target protein kinase. Hence, these reporters could improve the interpretation of HTS screening data by readily eliminating false-positive hits.
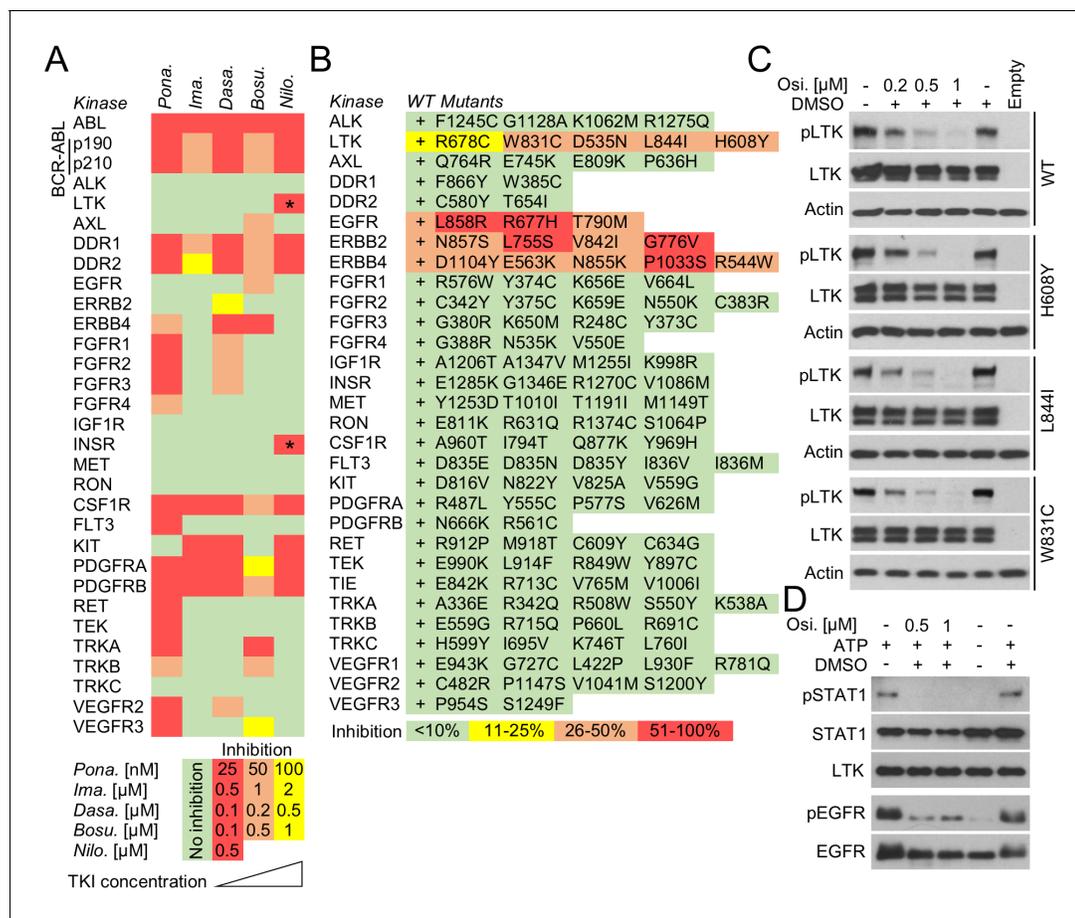
Figure 5. In-cell RTK activity profiling with BCR-ABL and EGFR inhibitors. (**A**) Activity of BCR-ABL inhibitors ponatinib (*Pona.*), imatinib (*Ima.*), dasatinib (*Dasa.*), bosutinib (*Bosu.*), and nilotinib (*Nilo.*) against 28 wild-type RTKs, evaluated in 293T cells transfected with RTKs and treated with inhibitors for 20–24 hr. The panel compiles data from immunoblot detections of activated RTKs, each treated with inhibitor concentrations derived from the experiments shown in *Figure 5—figure supplement 1*. Only one concentration is shown for nilotinib due to its cell toxicity at higher concentrations. Asterisks highlight the previously unreported nilotinib targets LTK and INSR (*Supplementary file 1E*; *Figure 5—figure supplement 1*). (**B**) Activity profiling of 30 wild-type (wt) RTKs and 116 of their active mutants in the presence of 0.5 µM osimertinib. 293T cells were transfected with RTK vectors together with pKrox24(2xD-E_inD)^{Luc}24 hr before osimertinib treatment (for 24 hr). The colors reflect the osimertinib-mediated inhibition of pKrox24(2xD-E_inD)^{Luc}*trans*-activation induced by a given RTK, relative to cells untreated with osimertinib. Basal levels of osimetrinib-mediated inhibition of pKrox24 (2xD-E_inD)^{Luc} were obtained from cells transfected with empty plasmid and then subtracted from the data. (**C**) 293T cells were transfected with wt LTK or its mutants, and treated with osimertinib (Osi.) for 24 hr. The LTK autophosphorylation (p) reflect LTK activity. Total LTK and actin serve as loading controls. (**D**) Cell-free kinase assays were carried out with recombinant LTK or EGFR and osimertinib added to the kinase reaction. Phosphorylation (p) of a recombinant STAT1 and autophosphorylation was used to detect LTK and EGFR activation, respectively. Samples with omitted ATP serve as negative controls for kinase activity.

DOI: 10.7554/eLife.21536.015

The following figure supplement is available for figure 5:

Figure supplement 1. Analyses of cytotoxicity and kinase activities of BCR-ABL and EGFR inhibitors.

DOI: 10.7554/eLife.21536.016

Methods

Cell culture, transfection and luciferase reporter assay

NIH3T3 cells (RRID:CVCL_0594) and 293 T cells (RRID:CVCL_0063) were obtained from ATCC (Manassas, VA). hiPSC cell line AM13 was generated as described before (*Krutá et al., 2014*). hESC (CCTL14; RRID:CVCL_C860) cells were prepared as described before (*Dvorak et al., 2005*). RCS cells (RRID:CVCL_S122), KMS11 (RRID:CVCL_2989) and LP1 (RRID:CVCL_0012) cells were obtained as described before (*Krejci et al., 2010*). All used cell lines were routinely evaluated for mycoplasma

contamination using DAPI staining and confocal microscopy, and were mycoplasma free. Cells were propagated in DMEM media, supplemented with 10% FBS and antibiotics (Invitrogen, Carlsbad, CA). hESC and hiPSC cells were propagated in feeder-free conditions. For 293T growth assays, 3 × 10 cells were grown in 24-well tissue culture plates for 1 day, and the cells were treated with inhibitors. After 24 hr the cell numbers were determined by cell counter (Beckman Coulter, Brea, CA). Chemicals were obtained from the following manufacturers: FGF2, SCF, FLT3 ligand, VEGF (RnD Systems, Minneapolis, MN); collagen type 1 (Santa Cruz Biotechnology, Santa Cruz, CA); PD0325901 (Tocris Bioscience, Bristol, UK); ponatinib, imatinib, dasatinib, bosutinib, nilotinib, osimertinib, AZD1480, BGJ398 (Selleckchem, Houston, TX); heparin (Sigma-Aldrich, St. Louis, MO). Cells were transfected either by using FuGENE6 transfection reagent (Roche, Basel, Switzerland), polyethylenimine (Sigma-Aldrich) or electroporation with the Neon Transfection System (Invitrogen). For the luciferase reporter assay, cells were also transfected with a vector expressing firefly luciferase and a vector expressing *Renilla* luciferase under the control of a constant promoter (pRL-TK) at a 3/1 ratio. Luciferase signal was quantified 20–24 hr later using the Luciferase or Dual-Luciferase Reporter Assay (Promega, Madison, WI). Osimertinib screening in 293T cells was carried out with pKrox24(2xD-E)^{Luc}only, which was transfected at a 1/3 ratio together with the RTK-expressing vector. The cells were treated with 0.5 μM osimertinib 24 hr after transfection, and luciferase signal was determined 24 hr later.

Plasmid cloning and mutagenesis

Vectors (pcDNA3.1) carrying C-terminally V5-tagged RTKs were generated by cloning full-length human RTK cDNA into a pcDNA3.1/V5-His TOPO TA vector (Invitrogen). Site-directed mutagenesis was carried-out according to the manufacturer's protocol (Agilent, Santa Clara, CA). Vectors (pCR3.1) carrying N-terminally FLAG-tagged p190 and p210 variants of BCR-ABL were generated by cloning full-length human BCR-ABL p190 cDNA (source pSG5-P190) and full-length human BCR-ABL p210 cDNA (source Bcr/Abl P210LEF) into a pCR3.1 vector (Invitrogen) containing a PGNQNMDYKDDDDK amino acid coding sequence between BamHI and EcoRI in the multiple cloning site. The source vectors pSG5-P190 (Addgene, Cambridge, MA; plasmid #31285) and Bcr/Abl P210LEF (plasmid #38158) were a gift from Nora Heisterkamp (*Yi et al., 2008*; *Kweon et al., 2008*). Promoter regions of *EGR1*, *EGR2*, *RGS1*, *NR4A2* and *DUSP6* were amplified from hESC genomic DNA by PCR and ligated to a pGL4.17 vector (Promega). All EGR1 promoter fragments of different lengths (hEGR1-B - hEGR1-F) were amplified from hEGR1-A by PCR and inserted into vector pGL4.17. The construct pKrox24(1xD-E_inD)^{Luc} was prepared by inserting the active element D-E, amplified from hEGR1-A by PCR, into the hEGR1-D construct. pKrox24(2xD-E_inD)^{Luc} was obtained by cloning synthetic DNA corresponding to two copies of the active element D-E to KpnI site of the hEGR1-D construct. pKrox24(3xD-D2_inD)^{Luc} was obtained by cloning three copies of the active element D-D2 as a synthetic gene by KpnI into the hEGR1-D construct. pKrox24(MapErk)^{Luc} was prepared by inserting synthetic DNA corresponding to five copies of a designed MapErk sequence (listed in *Figure 1—figure supplement 6*) into KpnI, HindIII sites of the pGL4.26 vector (Promega). Two copies of synthetic DNA corresponding to element D-E were cloned into HindIII, SalI sites of pDsRed-Express-DrVector (Clontech) to obtain pKrox24(2xD-E)^{DsRed}. pKrox24(MapErk)^{DsRed} was prepared by cloning of five copies of designed MapErk sequence into EcoRI, BamHI sites of the pDsRed-Express-Dr vector. pKrox24(2xD-E)^{dTomato} and pKrox24(MapErk)^{dTomato} were generated by swapping of dTomato cDNA from ptdTomato Vector (Clontech) to pCLuc-Basic2 by HindIII,NotI and BamHI,NotI sites, respectively. 2xD-E element was cloned to pCLuc-Basic2 by EcoRI,EcoRV sites, MapErk element was cloned into EcoRI,XhoI sites. *Supplementary file 1C* lists all expression vectors used in the study; *Supplementary file 1F* lists all PCR primers with marked restriction sites used for plasmid generation.

Immunoblotting

Cells were harvested into the sample buffer (125 mM Tris-HCl pH 6.8, 20% glycerol, 4% SDS, 5% *β*-mercaptoethanol, 0.02% bromophenol blue). Samples were resolved by SDS-PAGE, transferred onto a PVDF membrane and visualized by chemiluminiscence (Thermo Scientific, Rockford, IL). *Supplementary file 1D* lists the antibodies used in the study. Kinase assays were performed with 200 ng of recombinant EGFR or LTK (SignalChem, Richmond, CA) in 50 μl of kinase buffer (60 mM

HEPES pH 7.5, 3 mM MgCl$_2$, 3 mM MnCl$_2$, 3 μM Na$_3$VO$_4$, 1.2 mM DTT) in the presence of 10 μM ATP for 60 min at 30°C. Recombinant STAT1 was from Cell Science (Newbury port, MA).

Live cell imaging

Time-lapse microscopy experiments with living cells were conducted using either an automated incubation microscope BioStation CT (Nikon, Tokio, Japan) or a confocal laser-scanning microscope Carl Zeiss LSM 700 (Carl Zeiss, Jena, Germany) equipped with an atmospheric chamber. Phase contrast and fluorescence signal images were automatically acquired every 15 min during a 24 hr time period. Images were then processed and analyzed in either Nikon BioStation CT or Carl Zeiss ZEN 2 software. Phase contrast and fluorescence images were exported into Microsoft Publisher for the preparation of publication figures.

Acknowledgements

Additional information

Funding

Author ORCIDs

Pavel Krejci, http://orcid.org/0000-0003-0618-9134

Additional files

Supplementary files

• Supplementary file 1. Supplementary tables containing (A) Commercial providers of RTK activity profiling; (B) Nucleotide sequences cloned into the promoterless pGL4.17 vector expressing firefly luciferase; (C) Expression vectors used in the study; (D) Antibodies used in the study; (E) Literature survey of anti-RTK activity of BCR-ABL TKIs; (F) Primers used for reporter construction.
DOI: 10.7554/eLife.21536.017

• Supplementary file 2. Supplementary file contains numerical data for *Figure 1A,B,C,D and E*; *Figure 1—figure supplements 3*, *4*, *5A, B*, *7A and B*; and *Figure 5—figure supplement 1*.
DOI: 10.7554/eLife.21536.018

• Supplementary file 3. Supplementary file contains numerical data for *Figure 5B*.
DOI: 10.7554/eLife.21536.019

References

Bae JH, Schlessinger J. 2010. Asymmetric tyrosine kinase arrangements in activation or autophosphorylation of receptor tyrosine kinases. *Molecules and Cells* **29**:443–448. doi: 10.1007/s10059-010-0080-5, PMID: 20432069

Bamborough P. 2012. System-based drug discovery within the human kinome. *Expert Opinion on Drug Discovery* **7**:1053–1070. doi: 10.1517/17460441.2012.724056, PMID: 22971083

Buchtova M, Oralova V, Aklian A, Masek J, Vesela I, Ouyang Z, Obadalova T, Konecna Z, Spoustova T, Pospisilova T, Matula P, Varecha M, Balek L, Gudernova I, Jelinkova I, Duran I, Cervenkova I, Murakami S, Kozubik A, Dvorak P, et al. 2015. Fibroblast growth factor and canonical WNT/β-catenin signaling cooperate in suppression of chondrocyte differentiation in experimental models of FGFR signaling in cartilage. *Biochimica et Biophysica Acta (BBA) - Molecular Basis of Disease* **1852**:839–850. doi: 10.1016/j.bbadis.2014.12.020

Carter EP, Fearon AE, Grose RP. 2015. Careless talk costs lives: fibroblast growth factor receptor signalling and the consequences of pathway malfunction. *Trends in Cell Biology* **25**:221–233. doi: 10.1016/j.tcb.2014.11.003, PMID: 25467007

Cortes JE, Kim DW, Pinilla-Ibarz J, le Coutre P, Paquette R, Chuah C, Nicolini FE, Apperley JF, Khoury HJ, Talpaz M, DiPersio J, DeAngelo DJ, Abruzzese E, Rea D, Baccarani M, Müller MC, Gambacorti-Passerini C, Wong S, Lustgarten S, Rivera VM, et al. 2013. A phase 2 trial of ponatinib in Philadelphia chromosome-positive leukemias. *New England Journal of Medicine* **369**:1783–1796. doi: 10.1056/NEJMoa1306494, PMID: 24180494

Cox AD, Fesik SW, Kimmelman AC, Luo J, Der CJ. 2014. Drugging the undruggable RAS: Mission possible? *Nature Reviews Drug Discovery* **13**:828–851. doi: 10.1038/nrd4389, PMID: 25323927

Cross DA, Ashton SE, Ghiorghiu S, Eberlein C, Nebhan CA, Spitzler PJ, Orme JP, Finlay MR, Ward RA, Mellor MJ, Hughes G, Rahi A, Jacobs VN, Red Brewer M, Ichihara E, Sun J, Jin H, Ballard P, Al-Kadhimi K, Rowlinson R, et al. 2014. AZD9291, an irreversible EGFR TKI, overcomes T790M-mediated resistance to EGFR inhibitors in lung cancer. *Cancer Discovery* **4**:1046–1061. doi: 10.1158/2159-8290.CD-14-0337, PMID: 24893891

Dvorak P, Dvorakova D, Koskova S, Vodinska M, Krekac D, Hampl A. 2005. Expression and potential role of fibroblast growth factor 2 and its receptors in human embryonic stem cells. *Stem Cells* **23**: 1200–1211. doi: 10.1634/stemcells.2004-0303, PMID: 15955829

Finlay MR, Anderton M, Ashton S, Ballard P, Bethel PA, Box MR, Bradbury RH, Brown SJ, Butterworth S, Campbell A, Chorley C, Colclough N, Cross DA, Currie GS, Grist M, Hassall L, Hill GB, James D, James M, Kemmitt P, et al. 2014. Discovery of a potent and selective EGFR inhibitor (AZD9291) of both sensitizing and T790M resistance mutations that spares the wild type form of the receptor. *Journal of Medicinal Chemistry* **57**: 8249–8267. doi: 10.1021/jm500973a, PMID: 25271963

Forbes SA, Beare D, Gunasekaran P, Leung K, Bindal N, Boutselakis H, Ding M, Bamford S, Cole C, Ward S, Kok CY, Jia M, De T, Teague JW, Stratton MR, McDermott U, Campbell PJ. 2015. COSMIC: exploring the world's knowledge of somatic mutations in human cancer. *Nucleic Acids Research* **43**:D805–D811. doi: 10.1093/nar/gku1075, PMID: 25355519

Fountas A, Diamantopoulos LN, Tsatsoulis A. 2015. Tyrosine kinase inhibitors and diabetes: A novel treatment paradigm? *Trends in Endocrinology & Metabolism* **26**:643–656. doi: 10.1016/j.tem.2015.09.003, PMID: 26492 832

Greig SL. 2016. Osimertinib: first global approval. *Drugs* **76**:263–273. doi: 10.1007/s40265-015-0533-4, PMID: 26729184

Harskamp LR, Gansevoort RT, van Goor H, Meijer E. 2016. The epidermal growth factor receptor pathway in chronic kidney diseases. *Nature Reviews Nephrology* **12**:496–506. doi: 10.1038/nrneph.2016.91, PMID: 27374 915

Hochhaus A, Baccarani M, Deininger M, Apperley JF, Lipton JH, Goldberg SL, Corm S, Shah NP, Cervantes F, Silver RT, Niederwieser D, Stone RM, Dombret H, Larson RA, Roy L, Hughes T, Müller MC, Ezzeddine R, Countouriotis AM, Kantarjian HM. 2008. Dasatinib induces durable cytogenetic responses in patients with chronic myelogenous leukemia in chronic phase with resistance or intolerance to imatinib. *Leukemia* **22**:1200–1206. doi: 10.1038/leu.2008.84, PMID: 18401416

Hucthagowder V, Meyer R, Mullins C, Nagarajan R, DiPersio JF, Vij R, Tomasson MH, Kulkarni S. 2012. Resequencing analysis of the candidate tyrosine kinase and RAS pathway gene families in multiple myeloma. *Cancer Genetics* **205**:474–478. doi: 10.1016/j.cancergen.2012.06.007, PMID: 22939401

Inglés-Prieto Á, Reichhart E, Muellner MK, Nowak M, Nijman SM, Grusch M, Janovjak H. 2015. Light-assisted small-molecule screening against protein kinases. *Nature Chemical Biology* **11**:952–954. doi: 10.1038/nchembio.1933, PMID: 26457372

Jiang T, Zhou C. 2014. Clinical activity of the mutant-selective EGFR inhibitor AZD9291 in patients with EGFR inhibitor-resistant non-small cell lung cancer. *Translational Lung Cancer Research* **3**:370–372. doi: 10.3978/j.issn.2218-6751.2014.08.02, PMID: 25806323

Kant SG, Cervenkova I, Balek L, Trantirek L, Santen GW, de Vries MC, van Duyvenvoorde HA, van der Wielen MJ, Verkerk AJ, Uitterlinden AG, Hannema SE, Wit JM, Oostdijk W, Krejci P, Losekoot M. 2015. A novel variant of FGFR3 causes proportionate short stature. *European Journal of Endocrinology* **172**:763–770. doi: 10.1530/EJE-14-0945, PMID: 25777271

Krejci P, Murakami S, Prochazkova J, Trantirek L, Chlebova K, Ouyang Z, Aklian A, Smutny J, Bryja V, Kozubik A, Wilcox WR. 2010. NF449 is a novel inhibitor of fibroblast growth factor receptor 3 (FGFR3) signaling active in chondrocytes and multiple myeloma cells. *Journal of Biological Chemistry* **285**:20644–20653. doi: 10.1074/jbc.M109.083626, PMID: 20439987

Krejci P, Pejchalova K, Wilcox WR. 2007. Simple, mammalian cell-based assay for identification of inhibitors of the Erk MAP kinase pathway. *Investigational New Drugs* **25**:391–395. doi: 10.1007/s10637-007-9054-7, PMID: 17458503

Krutá M, Šeneklová M, Raška J, Salykin A, Zerzánková L, Pešl M, Bártová E, Franek M, Baumeisterová A, Košková S, Neelsen KJ, Hampl A, Dvořák P, Rotrekl V. 2014. Mutation frequency dynamics in HPRT locus in culture-adapted human embryonic stem cells and induced pluripotent stem cells correspond to their differentiated counterparts. *Stem Cells and Development* **23**:2443–2454. doi: 10.1089/scd.2013.0611, PMID: 24836366

Kubo T, Kuroda Y, Shimizu H, Kokubu A, Okada N, Hosoda F, Arai Y, Nakamura Y, Taniguchi H, Yanagihara K, Imoto I, Inazawa J, Hirohashi S, Shibata T. 2009. Resequencing and copy number analysis of the human tyrosine kinase gene family in poorly differentiated gastric cancer. *Carcinogenesis* **30**:1857–1864. doi: 10.1093/carcin/bgp206, PMID: 19734198

Kweon SM, Cho YJ, Minoo P, Groffen J, Heisterkamp N. 2008. Activity of the Bcr GTPase-activating domain is regulated through direct protein/protein interaction with the Rho guanine nucleotide dissociation inhibitor. *Journal of Biological Chemistry* **283**:3023–3030. doi: 10.1074/jbc.M705513200, PMID: 18070886

Laederich MB, Horton WA. 2012. FGFR3 targeting strategies for achondroplasia. *Expert Reviews in Molecular Medicine* **14**:e11. doi: 10.1017/erm.2012.4, PMID: 22559284

Lemmon MA, Schlessinger J. 2010. Cell signaling by receptor tyrosine kinases. *Cell* **141**:1117–1134. doi: 10.1016/j.cell.2010.06.011, PMID: 20602996

Loots GG, Ovcharenko I. 2004. rVISTA 2.0: evolutionary analysis of transcription factor binding sites. *Nucleic Acids Research* **32**:W217–W221. doi: 10.1093/nar/gkh383, PMID: 15215384

Meloche S, Pouysségur J. 2007. The ERK1/2 mitogen-activated protein kinase pathway as a master regulator of the G1- to S-phase transition. *Oncogene* **26**:3227–3239. doi: 10.1038/sj.onc.1210414, PMID: 17496918

Modugno M. 2014. New resistance mechanisms for small molecule kinase inhibitors of Abl kinase. *Drug Discovery Today: Technologies* **11**:5–10. doi: 10.1016/j.ddtec.2013.12.001

Naski MC, Wang Q, Xu J, Ornitz DM. 1996. Graded activation of fibroblast growth factor receptor 3 by mutations causing achondroplasia and thanatophoric dysplasia. *Nature Genetics* **13**:233–237. doi: 10.1038/ng0696-233, PMID: 8640234

Ni Q, Titov DV, Zhang J. 2006. Analyzing protein kinase dynamics in living cells with FRET reporters. *Methods* **40**:279–286. doi: 10.1016/j.ymeth.2006.06.013, PMID: 16908183

Notredame C, Higgins DG, Heringa J. 2000. T-Coffee: a novel method for fast and accurate multiple sequence alignment. *Journal of Molecular Biology* **302**:205–217. doi: 10.1006/jmbi.2000.4042, PMID: 10964570

Passos-Bueno MR, Wilcox WR, Jabs EW, Sertié AL, Alonso LG, Kitoh H. 1999. Clinical spectrum of fibroblast growth factor receptor mutations. *Human Mutation* **14**:115–125. doi: 10.1002/(SICI)1098-1004(1999)14:2<115::AID-HUMU3>3.0.CO;2-2, PMID: 10425034

Regot S, Hughey JJ, Bajar BT, Carrasco S, Covert MW. 2014. High-sensitivity measurements of multiple kinase activities in live single cells. *Cell* **157**:1724–1734. doi: 10.1016/j.cell.2014.04.039, PMID: 24949979

Scuto A, Krejci P, Popplewell L, Wu J, Wang Y, Kujawski M, Kowolik C, Xin H, Chen L, Wang Y, Kretzner L, Yu H, Wilcox WR, Yen Y, Forman S, Jove R. 2011. The novel JAK inhibitor AZD1480 blocks STAT3 and FGFR3 signaling, resulting in suppression of human myeloma cell growth and survival. *Leukemia* **25**:538–550. doi: 10.1038/leu.2010.289, PMID: 21164517

ten Freyhaus H, Dumitrescu D, Berghausen E, Vantler M, Caglayan E, Rosenkranz S. 2012. Imatinib mesylate for the treatment of pulmonary arterial hypertension. *Expert Opinion on Investigational Drugs* **21**:119–134. doi: 10.1517/13543784.2012.632408, PMID: 22074410

Vogelstein B, Papadopoulos N, Velculescu VE, Zhou S, Diaz LA, Kinzler KW. 2013. Cancer genome landscapes. *Science* **339**:1546–1558. doi: 10.1126/science.1235122, PMID: 23539594

Wang B, Chen J, Santiago FS, Janes M, Kavurma MM, Chong BH, Pimanda JE, Khachigian LM. 2010. Phosphorylation and acetylation of histone H3 and autoregulation by early growth response 1 mediate interleukin 1beta induction of early growth response 1 transcription. *Arteriosclerosis, Thrombosis, and Vascular Biology* **30**:536–545. doi: 10.1161/ATVBAHA.109.193821, PMID: 20018936

Wendt DJ, Dvorak-Ewell M, Bullens S, Lorget F, Bell SM, Peng J, Castillo S, Aoyagi-Scharber M, O'Neill CA, Krejci P, Wilcox WR, Rimoin DL, Bunting S. 2015. Neutral endopeptidase-resistant C-type natriuretic peptide variant represents a new therapeutic approach for treatment of fibroblast growth factor receptor 3-related dwarfism. *Journal of Pharmacology and Experimental Therapeutics* **353**:132–149. doi: 10.1124/jpet.114.218560, PMID: 25650377

Yang SH, Sharrocks AD, Whitmarsh AJ. 2003. Transcriptional regulation by the MAP kinase signaling cascades. *Gene* **320**:3–21. doi: 10.1016/S0378-1119(03)00816-3, PMID: 14597384

Yi SJ, Lee HT, Groffen J, Heisterkamp N. 2008. Bcr/Abl P190 interaction with Spa-1, a GTPase activating protein for the small GTPase Rap1. *International Journal of Molecular Medicine* **22**:453–458. doi: 10.3892/ijmm_00000042, PMID: 18813851

Yosaatmadja Y, Silva S, Dickson JM, Patterson AV, Smaill JB, Flanagan JU, McKeage MJ, Squire CJ. 2015. Binding mode of the breakthrough inhibitor AZD9291 to epidermal growth factor receptor revealed. *Journal of Structural Biology* **192**:539–544. doi: 10.1016/j.jsb.2015.10.018, PMID: 26522274

Zhao X, Ghaffari S, Lodish H, Malashkevich VN, Kim PS. 2002. Structure of the Bcr-Abl oncoprotein oligomerization domain. *Nature structural biology* **9**:117–120. doi: 10.1038/nsb747, PMID: 11780146